Estimating Seasonal Changes in Volumetric Soil Water Content at Landscape Scales in a Savanna Ecosystem Using Two-Dimensional Resistivity Profiling

Diana C. Garcia-Montiel*

Departamento de Ecologia Universidade de Brasilia, Brasilia, Brazil, and The Woods Hole Research Center, Falmouth, Massachusetts

Michael T. Coe

The Woods Hole Research Center, Falmouth, Massachusetts

Meyr P. Cruz

Departamento de Ecologia Universidade de Brasilia, Brasilia, Brazil

Joice N. Ferreira

Departamento de Ecologia Universidade de Brasilia, Brasilia, and EMBRAPA-Amazônia Oriental, Belém, Pará, Brazil

Euzebio M. da Silva

EMBRAPA-Cerrados, Planaltina, DF, Brazil

* Corresponding author address: Diana C. Garcia-Montiel, Department of Biology, University of Puerto Rico, Mayagüez Campus, P.O. Box 9012, Mayagüez, PR 00681-9012.
E-mail address: dgarcia@uprm.edu

DOI: 10.1175/2007EI238.1

Eric A. Davidson

The Woods Hole Research Center, Falmouth, Massachusetts

Received 6 June 2007; accepted 3 October 2007

ABSTRACT: Water distributed in deep soil reservoirs is an important factor determining the ecosystem structure of water-limited environments, such as the seasonal tropical savannas of South America. In this study a two-dimensional (2D) geoelectrical profiling technique was employed to estimate seasonal dynamics of soil water content to 10-m depth along transects of 275 m in savanna vegetation during the period between 2002 and 2006. Methods were developed to convert resistivity values along these 2D resistivity profiles into volumetric water content (VWC) by soil depth. The 2D resistivity profiles revealed the following soil and aquifer structure characterizing the underground environment: 0–4 m of permanently unsaturated and seasonally droughty soil, less severely dry unsaturated soil at about 4–7 m, nearly permanently saturated soil between 7 and 10 m, mostly impermeable saprolite interspaced with fresh bedrock of parent material at about 10–30 m, and a region of highly conductive water-saturated material at 30 m and below. Considerable spatial variation of these relative depths is clearly demonstrated along the transects. Temporal dynamics in VWC indicate that the active zone of water uptake is predominantly at 0–7 m, and follows the seasonal cycles of precipitation and evapotranspiration. Uptake from below 7 m may have been critical for a short period near the beginning of the rainy season, although the seasonal variations in VWC in the 7–10-m layer are relatively small and lag the surface water recharge for about 6 months. Calculations using a simple 1-box water balance model indicate that average total runoff was 15–25 mm month^{-1} in the wet season and about 6–9 mm month^{-1} in the dry season. Modeled ET was about 75–85 mm month^{-1} in the wet season and 20–25 mm month^{-1} in the dry season. Variation in basal area and tree density along one transect was positively correlated with VWC of the 0–3-m and 0–7-m soil depths, respectively, during the wettest months. These multitemporal measurements demonstrate that the along-transect spatial differences in soil moisture are quasi-permanent and influence vegetation structure at the scale of tens to hundreds of meters.

KEYWORDS: Two-dimensional (2D) resistivity profiling; Cerrado; Tropical savannas; Water-limited ecosystems; Water budgets

1. Introduction

Water present in deep soil may be essential for the maintenance of seasonal tropical savannas, where rates of potential evapotranspiration (PET) exceed precipitation during dry seasons that last several months (Frost et al. 1986). Water distributed in deep soil reservoirs has been extensively debated as one of the factors determining the structure of savanna vegetation and maintaining the hydrological cycles of these ecosystems affected by pronounced dry periods (Rawitscher 1948; Furley and Ratter 1988; Oliveira-Filho et al. 1989; Medina 1993). The reliance of these ecosystems on deep soil water depends on a combination of factors that include the distribution of soil structural features that determine plant

accessibility to water in these reservoirs, the length of dry periods, and the stochastic behavior of rain events during the wet periods (Frost et al. 1986). Above- and belowground vascular architecture of vegetation also determines plant accessibility to deep soil water.

Deep soil water has been measured or inferred at point locations in many ecosystem types using neutron probes, time domain reflectometry, or isotopic analyses (Jipp et al. 1998; Nepstad et al. 1994; Hodnett et al. 1995; Jackson et al. 1999; Moreira et al. 2003; Oliveira et al. 2005), but spatial heterogeneity of the belowground environment is difficult to assess with these methods. In spite of the critical role played by deep soil water in determining structure of many water-limited ecosystems, we lack methodologies that provide reliable estimates of soil plant-available water at landscape scales relevant to variation in plant communities (tens to thousands of meters). To address this problem, we applied a two-dimensional (2D) geoelectrical profiling technique as a tool to estimate seasonal dynamics of soil water content to 10-m depth along transects of 275 m in the Brazilian savanna locally known as "cerrado." The 2D geoelectrical profiling technique gained popularity during the 1990s, when a large effort was invested in developing a tool to map areas with moderately complex geology (Griffiths and Barker 1993). The objective was to detect lateral and vertical variations in electric resistivity caused by differences in soil texture and structure of materials. The technique has been successfully used in environmental (Jackson et al. 2005; Tabbagh et al. 2000), geological (Seaton and Burbey 2002), and archeological studies (Shaaban and Shaaban 2001). It has been particularly valuable for groundwater and fluctuating water table determinations (Seaton and Burbey 2002) and to investigate spatial and temporal variability of soil physical properties such as structure, fluid composition, and water content (Samouëlian et al. 2005). Because soil electrical resistivity is particularly sensitive to water characteristics of textural and structural materials, it provides a tool for soil water determinations along the soil profile (Sheets and Hendrickx 1995).

Measurements of soil resistivity consist of injecting a continuous current into the ground through two current electrodes (C1 and C2) and measuring the resulting voltage difference in two other potential electrodes (P1 and P2). Voltage and current measurements are obtained from an array of electrodes placed on the ground surface along a line of measure (Ojelabi et al. 2002; Seaton and Burbey 2002; Samouëlian et al. 2005). The assignment of currents and potentials electrodes at each point measurement is determined by a specific electrode configuration moving along the measured line. An apparent resistivity value is then calculated by knowing the intensity of the injected current (I), the difference in voltage (ΔV), and the geometric positions of the electrodes C1, C2, P1, and P2, determined by the array of the electrodes. The true resistivity values are then determined with an inversion of the apparent resistivity values using computerized inversion programs. The resultant product is a two-dimensional Earth model of resistivity distribution in the subsurface environment (Loke and Barker 1996).

Our primary objective in this study was to explore the potential of using resistivity profiling to estimate spatial and seasonal variation of water content of soil within the deep rooting zone (about 10 m) under savanna vegetation. We developed methods to convert resistivity values along 275-m transects into volumetric water content across the transects by soil depth increment and by month. In a

previous paper, spatial heterogeneity across these transects, measured once in each season, was evaluated through analysis of spatial autocorrelation of both soil water and vegetation structure (Ferreira et al. 2007). Spatial variation of selected vegetation attributes in one of the transects was similar to the spatial variation of soil water in the top 4 m. Comparisons with null models indicated that plants were randomly distributed over the wettest transect with the lowest heterogeneity in soil water, and clustered in the driest and most heterogeneous transect. Here, we detail the use of this methodology and describe the underlying geomorphic and soil features revealed by the 2D resistivity profiling. We also use monthly estimates of VWC and a simple water balance 1-box model to investigate changes in individual components of the water balance, that is, rates of evapotranspiration and runoff associated with the seasonality of the cerrado ecosystem. Finally, we explore relationships between spatial and temporal dynamics in VWC with measurements of the aboveground vegetation structure.

2. Study site

We conducted this study in selected areas of native cerrado located in the Ecological Station of Águas Emendadas [Estação Ecológica de Águas Emendadas (EEAE); Figure 1] 45 km northeast of Brasilia. The floristic physiognomy of this area is typical of the shrubby cerrado locally known as cerrado *stricto sensu* with characteristics of "dense cerrado" (Felfili and Silva 1993; Felfili et al. 2004). This type of physiognomy is typified in EEAE by the presence of woody vegetation with irregular and tortuous ramification, presenting an average height of ~2 m (Ferreira et al. 2007, specifically for the study area) and canopy cover between 50% and 70%. A 22-yr record indicates that mean annual precipitation is 1453 mm, with 90% of the rain falling between October and March, as represented by total monthly rainfall for the years 2002–06 (Figure 2). In this cerrado ecosystem the majority of the woody vegetation presents typical scleromorphic characteristics (Franco 2002), which increase their resistance to drought in this seasonal savanna.

The area of EEAE belongs to the central shield hydrogeological providence, which includes part of the Brasilia and Paraguai/Araguaia fold belt and part of the Amazon Craton (Mente 2000). Águas Emendadas belongs to the geomorphological unit known as Chapada, which comprises 34% of the area in the Distrito Federal. The Chapada region is usually associated with altitudes around 1000–1300 m above sea level and is characterized by flat to slightly undulating relief. The area covering the Distrito Federal is in general characterized by the presence of metamorphic rocks usually covered by a well-developed pedologic system, allowing the formation of porous or fractured aquifers (Lousada and Campos 2005). In EEAE the rock type attributed to the Paraná (97%) and Canastra (3%) groups (~1 billion years old) underlies the geology of the area (Lousada and Campos 2005). Metamorphic processes that occurred in the region [~650 million years ago (mya)] produced the extensive lateral plate movement that resulted in the foldings and fractures that formed the geological structures of the aquifers that characterize the hydrology of the ecological station (Lousada and Campos 2005).

Soils in the region are predominantly clayey (Figure 3), highly weathered Latossolos according to the Brazilian classification system (EMBRAPA 1999) or Acrustox according to the soil taxonomy (Soil Survey Staff 1999). The soils are

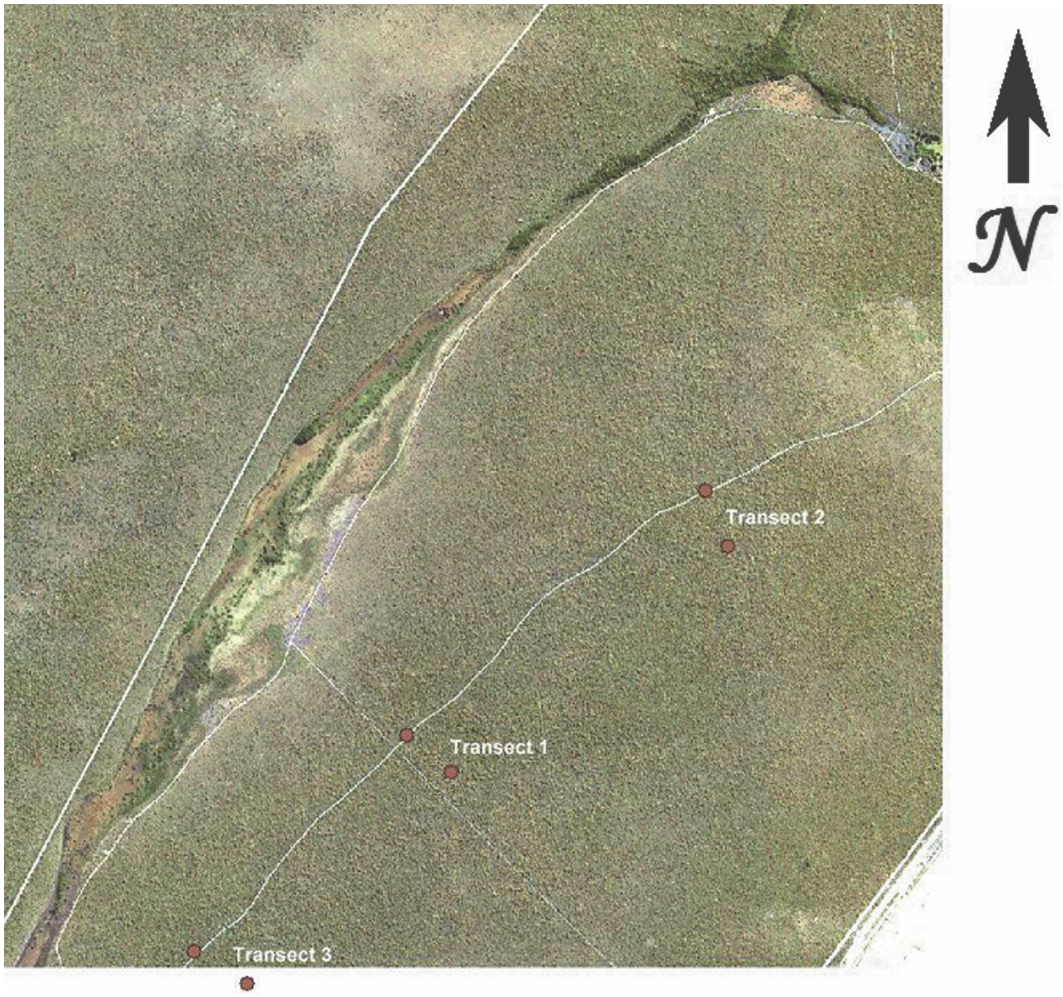

Figure 1. IKONOS image (6 Jun 2000) of Águas Emendadas area near Brasilia (Brazil) showing the location of transects along the study sites. Transect 1: (15°34′16.03″S, 47°35′34.29″W); transect 2: (15°33′36.79″S, 47°34′42.71″W); transect 3: (15°34′50.81″S, 47°36′10.45″W).

characterized by a high aggregate stability due to the large content of iron and aluminum oxides (Reatto et al. 1998; Motta et al. 2002). This physical property results in deep, well-drained soils. Some soil characteristics are shown in Figure 3.

3. Methods

Measurements of 2D resistivity profiling were conducted (i) 4 times during 2002 for calibration purposes along one 165-m transect covering an area where two 8-m-deep soil pits had been excavated and equipped with time domain reflectometry (TDR) probes; (ii) twice during 2003 for initial wet- and dry-season comparisons along three different 275-m transects (located at sites 1, 2, and 3)

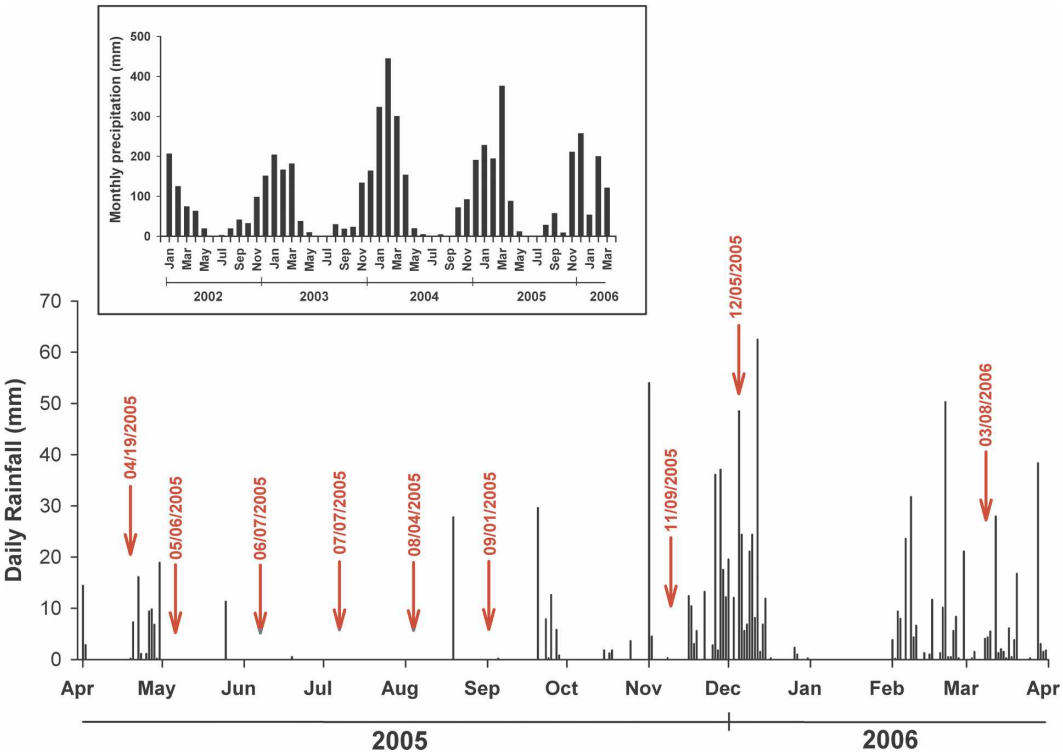

Figure 2. Total monthly rainfall for the years 2002–06 and daily precipitation for 2005–06. The source was the Chapada station of EMBRAPA-Cerrados (Centro de Pesquisas Agropecuárias do Cerrado) located (15°35′30″S, 47°42′30″W) close to the study sites in Águas Emendadas. Red titles indicate specific dates when resistivity measurements were conducted.

where detailed vegetation surveys were also performed; and (iii) 9 times during 2005 to obtain higher temporal measurement resolution along one of the 275-m transects (located at site 2) previously surveyed in 2003. All transects are within about 10-m elevation of each other. Based on surface observations, vegetation type, and topography, all transects appear to be replicates of a relatively homogeneous area within the EEAE landscape (Figure 1).

Resistivity profiles conducted along the shorter transect that included the soil pits with TDR probes were carried out during the months of January (middle of the wet season), March (end of wet season), April (transition between wet and dry season), and September (dry season), which provided a range of wetness values for calibration. This shorter 165-m transect was used to relate the resistivity measurements to volumetric water content (VWC) measured by TDR. Resistivity profiles along the three vegetation transects were conducted in the middle of the wet season in 17 February 2003 and at the end of the dry season in 15 October 2003. These two resistivity measurements from 2003 are used in this study to show the variation in soil water content associated with the spatial heterogeneity of the belowground environment. Resistivity profiles measured during 2005–06 were conducted on a monthly basis but only along transect 2. Previous measurements from

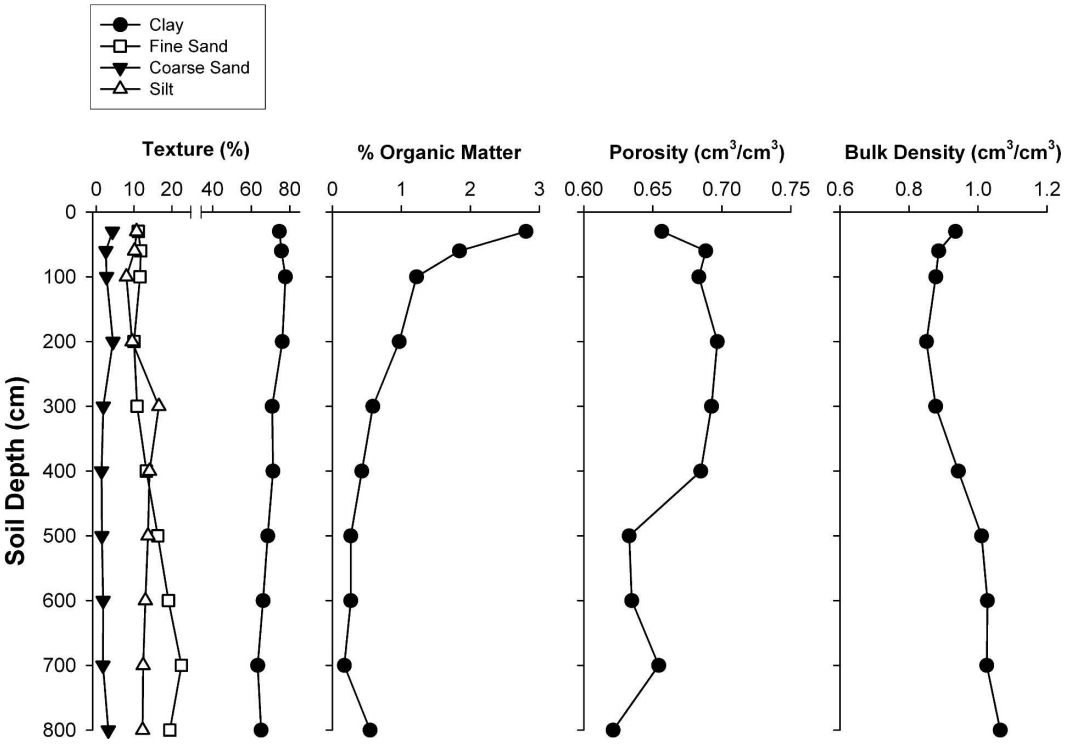

Figure 3. Soil characteristics of *cerrado denso* ecosystem in Águas Emendadas. Soil samples were obtained from the same 8-m soil pit equipped with TDR.

2003 showed that transect 2 presented the largest horizontal variation in VWC (discussed below) of the three transects. These monthly measurements were then used to investigate the dynamics of soil water content to a profile depth of 10 m together with changes in monthly runoff and evapotranspiration rates.

3.1. Two-dimensional resistivity profiling

Field resistivity measures were conducted with a commercially available Earth resistivity meter, the Sting R1 IP single-channel memory Earth resistivity connected to a Swift dual mode automatic multielectrode system (Advanced Geosciences, Inc). We employed a 56-electrode cable laid in a straight-line transect along the length of the profile (275-m transect) to be imaged. For all three vegetation transects, the electrode separation was 5 m for a maximum soil resistivity profile depth of about 37 m. For the resistivity profiles along the transect covering the TDR-instrumented soil pits, electrodes were laid out with a 3-m separation between them for a maximum profile depth of 23 m. Along all transects, individual electrodes were secured on the surface by stainless steel stakes inserted in the soil and equipped with a spring contact to hold the electrode.

The Wenner array configuration was used to assign current and potential electrode arrangements at each point measurement (Advanced Geosciences, Inc. 2004). This electrode configuration has been considered to produce a relatively

high resolution of horizontal structures and a good signal response (Sharma 1997) and has been suggested for research where a relatively shallow depth (<50 m) of investigation is required (Seaton and Burbey 2002). In addition, the fact that the Wenner array uses fewer point measurements compared to other arrays minimizes data acquisition time. The resistivity meter automatically and systematically selects combinations of current and potential electrodes along the line of measurement in order to target the different points at varying vertical and horizontal positions along a 2D profile and to measure resistivity in those specific points. Differences in duplicate resistivity measures taken at one data collection point of less than 5% were usually accepted. We automatically inverted field measurements of apparent resistivity with the inversion software EarthImager 2D developed by Advanced Geosciences, Inc. (Advanced Geosciences, Inc., 2004).

Once 2D resistivity profiles were constructed, resistivity values for specific soil depths were extracted by applying interpolation and data extraction techniques developed with the geographic information system (GIS) software IDRISI Kilimanjaro Version 14–02 (Eastman 2003). The raw inverted resistivity data were saved as universal resistivity data files that were then converted into IDRISI vector files using IDRISI conversion tools. A nonconstrained Delaunay triangulation was produced from the vector points of each imaged soil profile using the triangulated irregular network (TIN) model of the GIS software. The TIN facet attributes were then interpolated to generate a raster image from which resistivity values along specific depths were extracted. We extracted resistivity values at depths of 0, 30, and 100 cm and then at each meter up to a maximum depth of 10 m for the 275-m transects. For the 165-m transect we extracted resistivity values to a maximum depth of 8 m, the depth to which the soil pits were excavated and equipped with TDR.

3.2. Time Domain Reflectometry

The TDR technique relates the apparent dielectric constant of the soil to VWC (Topp et al. 1980). It was used here to monitor changes in volumetric soil water content within three 8-m-deep soil pits located along our short transect. TDR sensors consisted of 30-cm, parallel, stainless steel rods imbedded in the soil (Nepstad et al. 2002). At each pit, two vertical sensors were installed at the soil surface to measure VWC in the first 30 cm of soil depth. Horizontal sensors were installed in opposite walls to measure VWC at depths of 50 and 100 cm, and then at each meter up to a maximum depth of 8 m. To avoid the effects of evaporation through the soil pit wall, each horizontal sensor was installed at the end of a 1.5-m-long auger hole that had been drilled horizontally into the wall of the pit. After installing the TDR probe, the hole was then backfilled with soil. Measurements of VWC were made using a cable tester (Tektronix 1502C) and the calibration equation developed by Jipp et al. (Jipp et al. 1998) for an Oxisol. Resistivity measures near each soil pit were compared to VWC obtained through TDR on the same day that resistivity values were collected. Resistivity data points in the area of TDR measurements were obtained through the interpolation and data extraction techniques explained above. Regression analyses were used to develop a functional relationship to convert soil resistivity values for this soil type to VWC.

3.3. Vegetation survey

Vegetation was surveyed along each 275-m vegetation transect, by establishing continuous 10 m × 10 m plots centered around the odd-numbered electrodes, for a total sampled area of proximately 0.8 ha, within which 3500 woody trees were surveyed (see Ferreira 2006 for details on the vegetation survey). All woody stems equal to or greater than a 2.86-cm diameter (9-cm circumference) at 0.3 m from the ground level were measured, permanently tagged, and identified to the species level. Within all plots we measured diameter (at 0.3 m from the ground level) and height. Crown depth was calculated as the difference between tree height and the height to the first branch with green vegetation above the ground. Tree density was calculated as the number of individuals per 100 m^2. For this study we only report vegetation data obtained from transect 2.

3.4. Statistical methods

Statistical analysis was designed to explore potential relationships of monthly VWC with measured parameters describing the structure or phytosociologies of plant communities along transect 2. Ferreira et al. (Ferreira et al. 2007) investigated in detail the spatial autocorrelation of both soil water content and vegetation properties, and the results of simple correlation analyses reported here are consistent with those reported by Ferreira et al. (Ferreira et al. 2007). For the purpose of conducting correlation analysis, we calculated running averages of VWC for each plot to pair with the mean vegetation parameters estimated for vegetation plots. Because lateral roots within a single 10 m × 10 m plot (100 m^2) could draw on water reservoirs located from neighboring plots, the running VWC averages covered an area that expanded for another 5 m at each side of the 10 m × 10 m vegetation plots and in the direction of the transect, which provided a VWC plot area twice the length (20 m) of the vegetation plots. Correlation matrices of months and soil depths at 100-cm increments were constructed to find relationships between vegetation structural parameters and VWC at 100-cm increment soil depths. Where analysis of VWC estimates of 1-m soil depth increments indicated significant correlation with aboveground vegetation structural parameters, then the VWC values were summed for larger depth increments (e.g., 0–3, 0–6, 7–10 m) and again correlated with structural vegetation parameters. Statistical analyses were conducted using SYSTAT 9.0 (SPSS Science, Chicago, Illinois) with a datalog transformed when needed to meet the requirements of parametric statistics.

4. Results and discussion

4.1. Two-dimensional resistivity profiles

The 2D resistivity profiling of the underground environment of our study transects (Figure 4) revealed the large spatial and temporal variability that affects water distribution within the soil environment of the cerrado ecosystem. At all three transects measured during 17 February and 15 October 2003, the highest resistivity values (red to yellow colors) are observed in the first approximately 400 cm of land surface (Figure 4). The high resistivity values result from the low

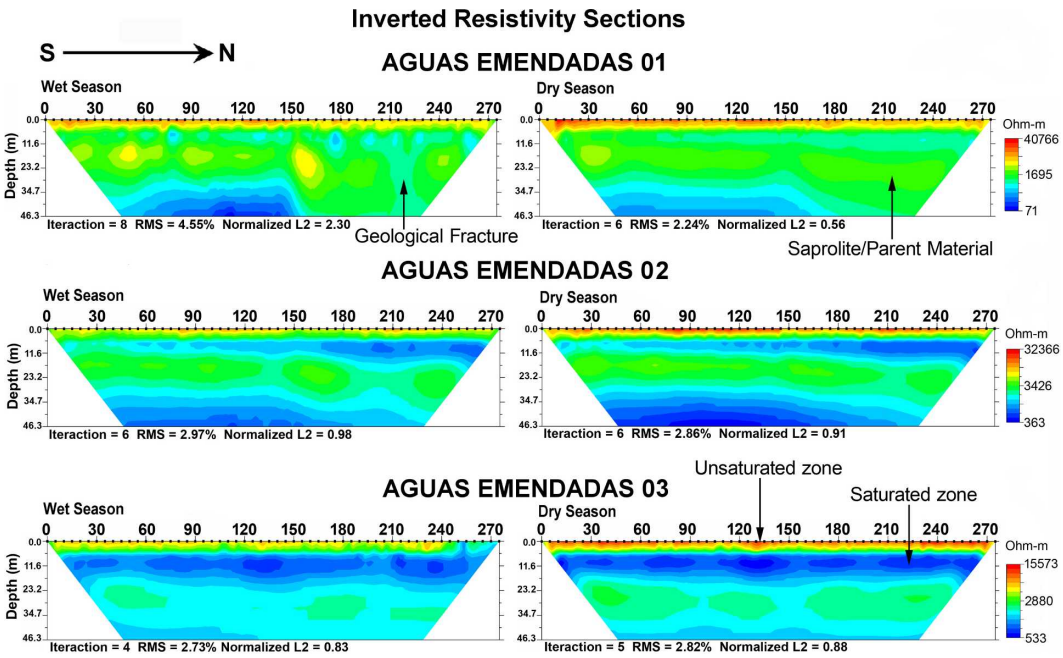

Figure 4. Inverted 2D resistivity Earth models for *cerrado denso* along transects in Águas Emendadas (Brazil). The 2D resistivity measurements were conducted during the middle of the wet season in 17 Feb 2003 and at the end of the dry season in 15 Oct 2003. Distance between electrodes was 5 m (for a transect of 275-m length) and measurements used Wenner configuration.

conductive conditions associated with the dryness of the soil surface, especially during the dry season in these seasonal tropical savannas. This nonsaturated, high resistivity zone observed at the top of the profiles is directly impacted by the seasonality of precipitation and evapotranspiration processes of the vegetation. Direct field observations showed that immediately below this dry region there is an additional nonsaturated zone of less severe dryness that extends for another 300–400 cm (green color). This zone appears in the 2D resistivity profiles as a transition interval between the upper low-conductive soil region and the highly conductive zone observed beneath, starting at about 700-cm depth, and is frequently observed along aquifers of similar characteristics (Lousada and Campos 2005). The presence of this transition interval is clearly observed along all three 2D resistivity profiles, but toward the southern end of transect at site 1 the highly conductive zone seems to be more fragmented near the surface, at least during the wet season. Taken as a whole, the first approximately 700 cm of the soil surface represents an area of unconsolidated material to which the water table never reaches, and therefore defines a soil region where nonsaturation conditions prevail.

In all three transects (Figure 4) soil resistivity profiles reveal a region below the unsaturated zone, starting at about 7–8 m, that is characterized by lower resistivity (higher conductivity) values, thus defining a zone of relatively permanent water-

saturated conditions. The soil depth up to which this second region extends shows remarkably significant horizontal variation along the sampled transects. In some cases, this high conductivity layer is less well defined, as can be observed toward the southern part of transect 1 during the wet season, where only pockets of blue shading can be observed between 8- and 14-m depth (Figure 4a). To the north side of this same transect, the depth of the saturated zone seems to reach about 16–18 m (blue shading). Transect 1 exhibits the least horizontal continuity in this lower resistivity zone. In transect 3, this same zone extends to depths of about 20 m in the middle part of the transect, and it also has the greatest continuity among the three transects (Figure 4c). The water in this zone of relatively permanently saturated conditions accumulates from gravitational infiltration of rainwater passing throughout a nonsaturated well-aerated zone, and stays perched over an impermeable bedrock material. These nonsaturated and permanently saturated regions comprise the unconsolidated material that defines total soil depth in the region. This soil reservoir of relatively shallow water characterizes the aquifer structure of EEAE (Lousada and Campos 2005) and is clearly exposed through our 2D resistivity profiles.

Another important feature exposed in each resistivity profile (Figure 4) is a horizontal layer of intermediate resistivity values, shown as various shades of green ranging from 15- to 35-m depth. This deep intermediate resistivity region represents the presence of an impermeable material over which the shallow water-saturated zone is suspended, which very likely corresponds to saprolite interspaced with fresh bedrock of parent material. Below the saprolite/bedrock, a region of lower resistivity values reappears and indicates the presence of a highly conductive water-saturated material at deeper soil depths (e.g., 30 m and below).

Because of the geological localization of the EEAE study area along the folding belt that resulted from past metamorphic activities, the presence of vertical transition zones associated with fracture planes within the bedrock is a common feature defining the hydrogeology of the area (Campos 2004). One of these zones is clearly exposed at the right end of the wet-season profile of transect 1 (Figure 4a) as a vertically aligned lower resistivity zone inserted across the saprolite/bedrock material. These fractured planes are usually filled with saturated material, very likely of argillic origin produced from weathering processes occurring along the fracture plane (Lousada and Campos 2005). When present, these fractures seem to connect the deeper saturated material with the shallow saturated zone (Figure 4a), and water from shallow reservoirs may eventually reach deeper regions of the aquifer by water infiltration through the porous material filling fracture planes along the bedrock. Vertical and horizontal anisotropy, in addition to precipitation and evapotranspiration, also control infiltration in this system. Similar features can be observed along transects 2 and 3 (Figures 4b,c). Overall, the depth, thickness, and internal distribution of the saprolite/bedrock and fractures seem to determine the major structural differences of the underground environment among the three transects, including distribution of water reservoirs, which are not apparent from aboveground observations.

4.2. Calibration of resistivity with TDR

Resistivity values extracted as close as possible to the TDR measurement positions were strongly correlated with TDR estimates of volumetric water content

across months and soil depths in the two soil pits within the short transect measured during 2002 (Figure 5a). The highest resistivity values were observed in the upper 400 cm of the soil (Figure 5a), consistent with the trends observed in surface resistivity distribution along the 2D resistivity profiles obtained in 2003 (Figure 4). The largest variation between months was also observed in the upper 400 cm of soil during September 2002, the end of the dry season (Figure 2), which shows the highest values in resistivity. As soil becomes wetter, resistivity values also decrease in the upper 400 cm of soil and down to 8 m. At soil depth below 4 m, the seasonal variation in soil resistivity values was relatively small. A polynomial relationship between the natural logarithm of resistivity and VWC measured by TDR was highly significant ($r^2 = 0.78$; $p < 0.001$). Based on this regression we derived a functional relationship [ln(Resistivity) = 10.882 – 0.004% VWC^2] to convert resistivity values into VWC for these soils of the EEAE study site.

Plant uptake of deep soil water in forests and woodlands on Oxisols has been inferred in previous studies conducted at point locations of soil pits (Jipp et al. 1998; Nepstad et al. 2002; Oliveira et al. 2005). In the study from Oliveira et al. (Oliveira et al. 2005) conducted in a cerrado ecosystem, TDR measurements of VWC were converted to plant-available water by calculating the difference between soil VWC and the residual soil water content at which roots can no longer extract water. These point estimates of plant-available water are then assumed to represent the water budget for the ecosystem. Our calculations of minimum dry-season VWC, however, indicate large spatial heterogeneity for the observed minimum residual soil water content, ranging from 9.5% VWC in transect 1 to 18.2% VWC in transect 3. In addition, our observations also suggested that the native vegetation is able to withdraw water from soil at matric potentials lower than the −1.5 MPa suggested for agricultural soils (Hodnett and Tomasella 2002), because the minimum dry-season VWC for all transects were frequently lower than the estimated residual VWC-values obtained throughout the traditional Van Genuchten (Van Genuchten 1980) parameterization based on laboratory water retention curves (data not shown). For the purpose of this study, we do not attempt to estimate plant-available water, but rather analyze our data as VWC estimated through calibration of resistivity values with TDR.

4.3. Temporal changes in volumetric water content

The active soil layer in this relatively low precipitation, high potential evapotranspiration environment is limited to the top about 700 cm of the soil column (Figure 6). Above 700-cm depth, the seasonal variation of the VWC is large, follows the seasonal cycles of precipitation and evapotranspiration, and decreases with increasing depth. In the 2005–06 water year, the difference between dry- and wet-season column-integrated $VWC_{0–700}$ is 311 mm, with the lowest $VWC_{0–700}$ value (1682 mm) recorded on 9 November and the greatest (1993 mm) on 8 March 2006 (Table 1). The net $VWC_{0–700}$ increases by 118 mm from the first measurement on 19 April 2005 to the last measurement on 8 March 2006. For the 700–1000-cm depth, the VWC is much greater per unit soil depth (about 300 mm m^{-1}), while the seasonal variation is relatively small (38 mm) and appears to lag the precipitation by about 6 months (maximum $VWC_{700–1000}$ in July–August and minimum $VWC_{700–1000}$ in December–March). The net $VWC_{700–1000}$ decreases by about 28 mm from April 2005 to March 2006 (Table 1).

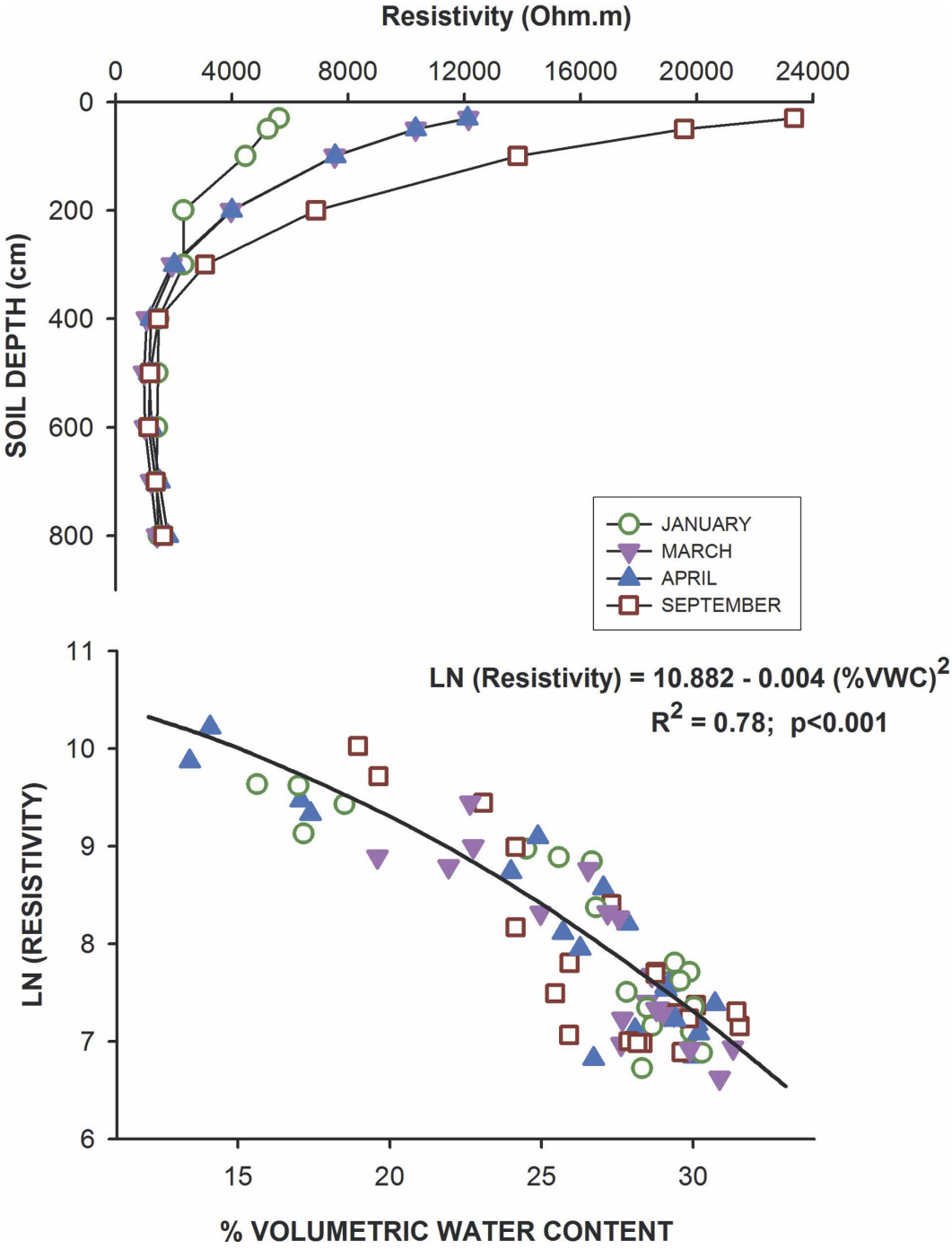

Figure 5. (a) Changes in resistivity along soil profile by month of measurement obtained from areas of soil pits located in Águas Emendadas equipped with TDR, and (b) relationship between resistivity values and soil moisture content measured with TDR among depths and dates.

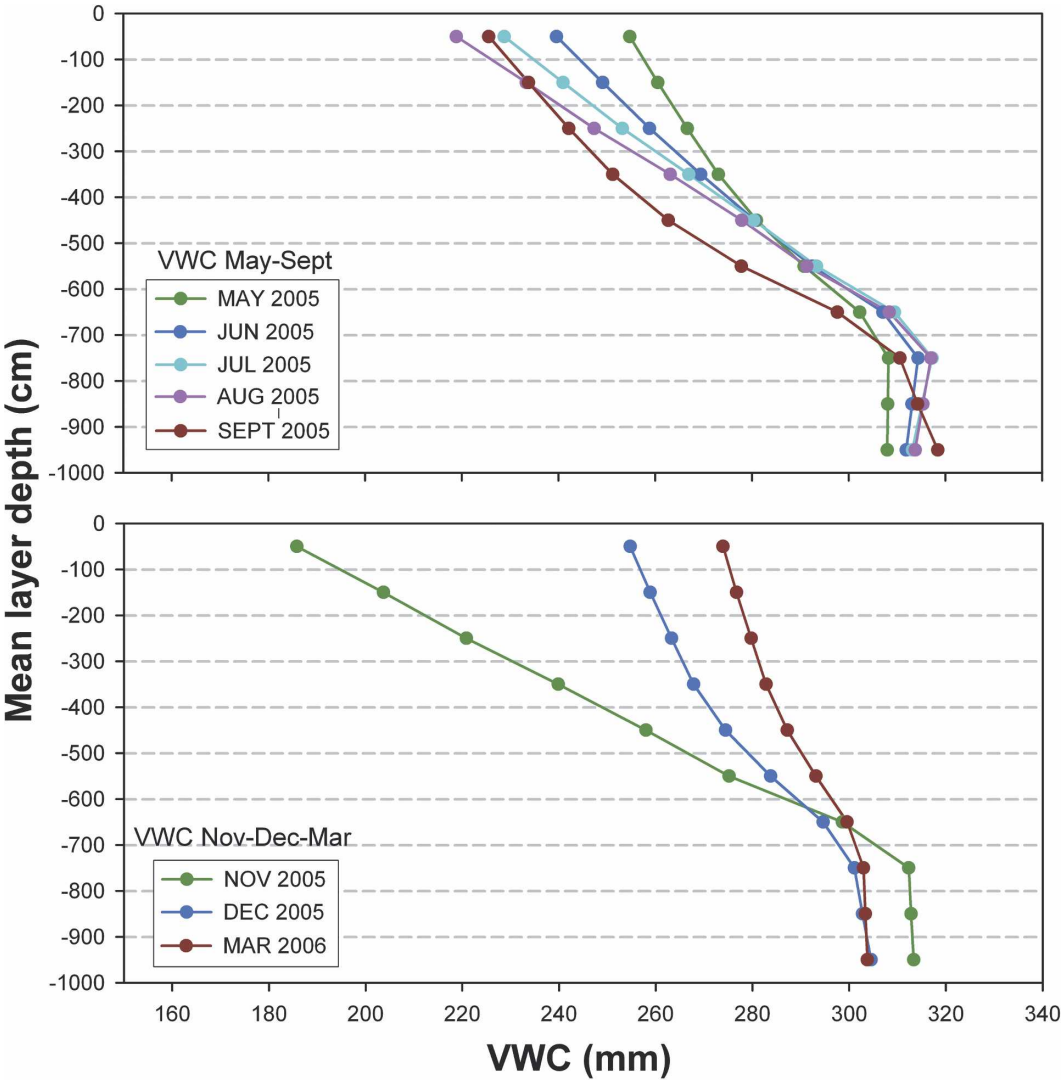

Figure 6. Profiles of mean VWC for transect 2- by 1-m soil depth increments and by month during 2005–06.

Changes in monthly precipitation and evapotranspiration rapidly influence the column-integrated volumetric water content of the top active soil layer (Figures 6 and 7). The onset of the dry season during the month of May starts the decline in soil water content, with a drop of about 32 mm from 6 May to 7 June, and 106 mm from 7 June to 5 September, the months of least precipitation (Figures 2 and 7; Table 1). The May–September decline in soil moisture is greatest in the upper 400 cm of the soil column (Figure 6), consistent with the previous observations from resistivity values measured during 2002 represented in Figure 4a. A further drop in $VWC_{0–700}$ of about 110 mm is observed from 5 September to 9 November, and it takes place in spite of about 124 mm of precipitation (Figure 7; Table 1).

The total evapotranspiration plus total runoff (ET+*R*) for a given period can be

Table 1. Monthly and annual mean water balance. VWC integrated for the soil layer 0–700 cm is shown in the second column (mm), *P* is the precipitation (mm) that occurred since the last VWC measurement, ET+*R* is calculated as the change in observed VWC minus precipitation that month, ET-Sim is simulated ET estimated based on rates of 0.75 mm day^{-1} in the dry season and 2.75 mm day^{-1} in the wet season, *R*-Sim is simulated total runoff based on rates of about 0.2 mm day^{-1} in the dry season and 0.47 mm day^{-1} in the wet season, VWC integrated for the soil layer 700–1000 cm is shown in the sixth column (mm), and simulated VWC integrated for the soil layer 0–700 cm is shown in last column (mm). No VWC measurements were made in October, January, and February so they are estimated as the average of neighboring months.

Date	$VWC_{0–700}$	*P*	ET+*R*	ET-Sim	*R*-Sim	$VWC_{700–1000}$	$VWC_{0–700}$Sim
19 Apr 2005	1875					938	1875
6 May 2005	1929	71	−17	−21	−5	924	1920
7 Jun 2005	1897	11	−43	−24	−7	939	1901
7 Jul 2005	1873	1	−24	−23	−6	946	1872
4 Aug 2005	1840	0	−33	−21	−6	946	1846
5 Sep 2005	1791	28	−77	−60	−12	943	1802
5 Oct 2005	1736	57	−112	−83	−15	941	1762
9 Nov 2005	1682	67	−122	−96	−17	938	1716
5 Dec 2005	1897	232	−17	−72	−13	908	1864
5 Jan 2006	1929	200	−168	−85	−17	909	1961
5 Feb 2006	1961	52	−20	−85	−17	909	1923
8 Mar 2006	1993	184	−152	−85	−17	910	1993
Annual	118	903	−785	−657	−130	−28	118

calculated as the difference in VWC from the previous measurement minus the precipitation that fell in that period. The total ET+*R* is 194 mm for the 4-month period from May to September and 234 mm for the 2 months from 5 September to 9 November (Table 1). That the total is much greater late in the dry season (September to November) than early in the dry season (June to September) suggests a higher evapotranspiration rate in the period September to November, since runoff is known to be very low at this time of year (Markewitz et al. 2006). This increased evapotranspiration rate late in the dry season is consistent with the observed increase in new leaf production that occurs before the wet season begins. The soil moisture in the top 1 m of the column increases slightly in September compared to August (consistent with increased rainfall) but decreases substantially between 200- and 700-cm depth (Figure 6), suggesting that deep root uptake of water was most important late in the dry season. *Kielmeyera coriacea*, which accounts for an average of 13% of all individuals across the three transects (Ferreira 2006), is a drought deciduous tree that produces new leaves before the end of the dry season, has high transpiration rates and high stomatal conductance, and has been shown to take up water from below 200-cm depth (Bucci et al. 2004; Jackson et al. 1999). Our data suggest that transpiration rates may increase late in the dry season, before there is sufficient rain to support this enhanced ET, and that soil water uptake from below 200 cm makes up the difference.

Although deep soil water uptake is notable from September to November, $VWC_{0–700}$ decreases in all layers, particularly drastically in the upper 4 m. This suggests that the shallow-rooted perennial grasses may also have begun to tran-

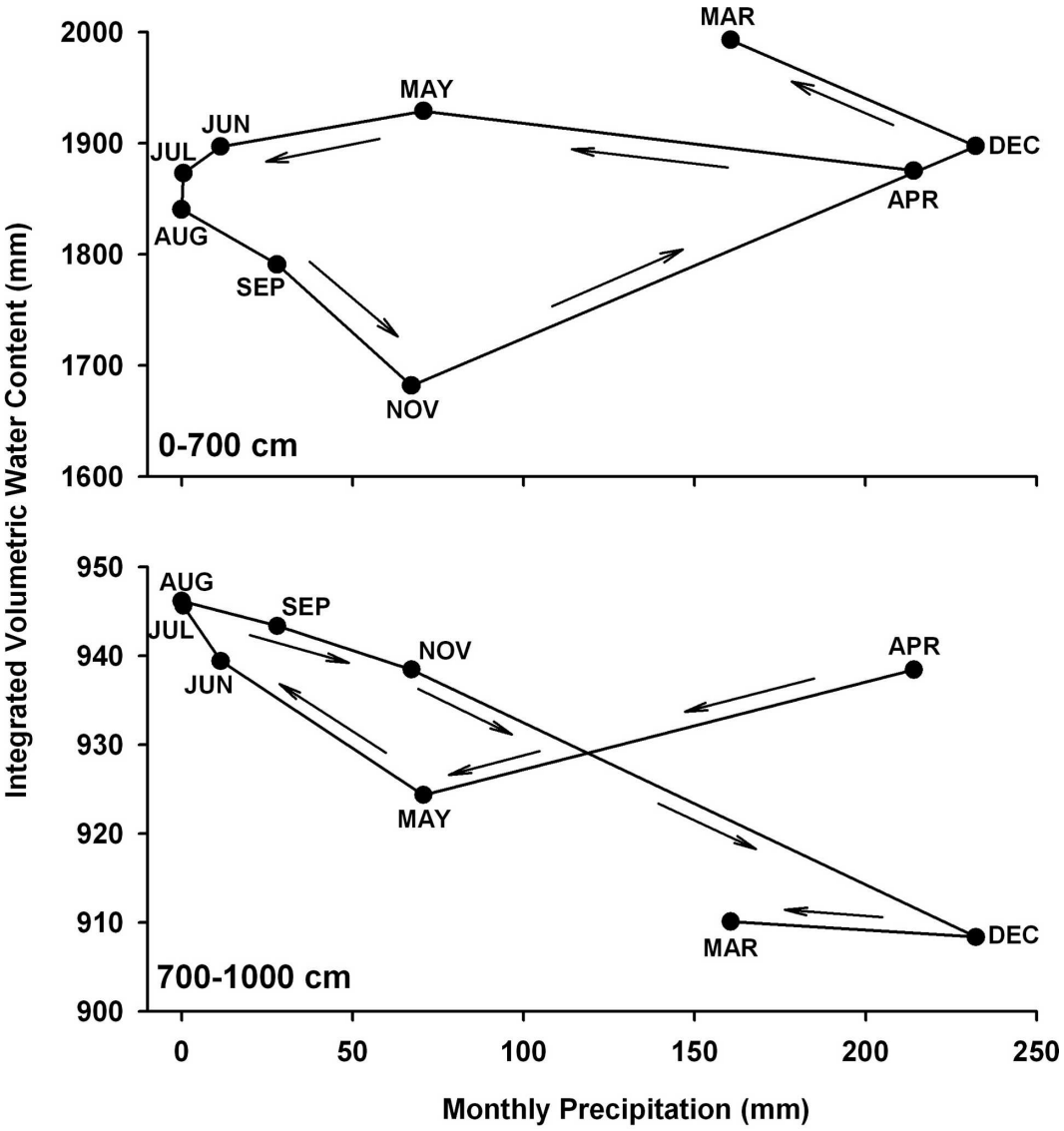

Figure 7. 2005–06 column-integrated VWC for the 0–700-cm and 700–1000-cm soil layers as function of monthly precipitation in Águas Emendadas. Values of VWC represent the average of all resistivity values along the 275-m transect measured at each month. All VWC values were obtained from resistivity measurements conducted during 2005, except for measurements from March, which were conducted in 2006.

spire at this time with the onset of the first rains of the season. After November there is a rapid recharge of soil water in the upper soil layer as precipitation exceeds evaporative demand, with an absolute increase of 311 mm by March.

In the 700–1000-cm soil layer, the observed variations in the column-integrated VWC are relatively small compared to the upper soil layer and lag the surface response by about 6 months, as indicated by the clockwise trend in water recharge

of the 700–1000-cm soil layer compared to the counterclockwise recharge pattern observed in the active 0–700-cm soil layer (Figure 7). A continuous drop in $\mathrm{VWC}_{700-1000}$ is observed from August to December and amounts to a total $\mathrm{VWC}_{700-1000}$ difference of 52 mm. No significant recharge occurs at the height of the wet season from December to March. Instead, the recharge phase in the lower layer occurs from May to August, consistent with decreased evaporative demand in the upper soil layers in the dry season and modest recharge from precipitation in the previous wet season. This observed lag to recharge the column-integrated 700–1000-cm soil layer has been previously documented by Oliveira et al. (Oliveira et al. 2005) in a study conducted in the *cerrado denso* located in the IBGE-RECOR Ecological Reserve, 70 km away from our study site in EEAE. Oliveira et al. (Oliveira et al. 2005) reported that after the onset of the wet season, it took about 100 days to recharge what they considered their deepest soil compartment (4–7.5 m). Our temporal sampling in the present study clearly indicates that it takes about 6 months to recharge soil water content of the 700–1000-cm soil reservoir (Figure 7).

To better understand the individual components of the water balance within the soil column we constructed a simple 1-box model of the form

$$d\mathrm{VWC}_{0-700}/dt = P - \mathrm{ET} - R,$$

$$\mathrm{VWC}_{0-700(f)} = \mathrm{VWC}_{0-700(t-1)} + d\mathrm{VWC}_{0-700(f)},$$

$$R = k\mathrm{VWC}_{0-700(t-1)},$$

where $d\mathrm{VWC}_{0-700}/dt$ is the change in time ($dt = 1$ day) of the volumetric water content, P is the measured precipitation, ET is the estimated evapotranspiration rate, and R is the sum of surface runoff and subsurface drainage rates (all in millimeters per day). Here R is calculated as the product of the volumetric water content and a prescribed drainage coefficient (k, day^{-1}).

We estimate ET and R (by modifying k) based on observations by Quesada et al. (Quesada et al. 2004) and Markewitz et al. (Markewitz et al. 2006) at the Roncador stream located within the IBGE-RECOR Ecological Reserve (with very similar *cerrado denso* vegetation) covering the period 1998–2000 and on flux tower data from Águas Emendadas for 2004 (A. J. B. Santos and L. M. Breyer, unpublished data). These sources of data suggest that ET varies from about 2.5–3 mm day^{-1} in the wet season and 0.25–0.75 mm day^{-1} in the dry season, and that R is perhaps as much as 25% of the annual precipitation rate. We define the dry season as beginning on 24 April after the last major rains and ending on 18 August shortly after a 28-mm rainfall event. The R and ET estimates were systematically varied and the equations solved for VWC_{0-700} for each day (t) from 19 April 2005 to 8 March 2006, starting with the observed VWC_{0-700} of 1875 mm. Accuracy is limited with a model this simple because ET and R are estimated simultaneously using observed values as a guide rather than being physically derived from a fully dynamic land surface model. Nonetheless, it serves as a useful tool for investigating the partitioning of the surface water budget. Several combinations of ET and R in the range of the observed values (ET of about 2.5–2.75 mm day^{-1} in the wet season and 0.675–0.75 mm day^{-1} in the dry season and R of 0.2–0.3 mm day^{-1} in the dry season and 0.47–0.85 mm day^{-1} in the wet season) result in a very good

fit ($r^2 > 0.986$) of the simulated $VWC_{0–700}$ to the observed (see Table 1 for one example).

The simulated $VWC_{0–700}$ increases by 118 mm from April 2005 to 8 March 2006 in agreement with the observations and the final value in March 2006 of 1993 mm is identical to the observed value (Table 1). The model suggests that for this period in which 903 mm of precipitation fell, about 15–25 mm month^{-1} of runoff was generated in the wet season and about 6–9 mm month^{-1} in the dry season. ET was about 75–85 mm month^{-1} in the wet season and 20–25 mm month^{-1} in the dry season. The agreement of the modeled monthly change in $VWC_{0–700}$ with the observed during the dry season is extremely good, being within ±12 mm of the observed value from April to September (Table 1).

The agreement in November and December is not as good (Table 1; +34 and −33 mm, respectively) reflecting perhaps rapid fluctuations of ET and *R* in response to short-term precipitation events, which are not included in this simple model. The lack of agreement in December may also be due, at least in part, to other factors not included in the model. An examination of the December observed water budget shows only 17 mm available for ET+*R* (compared to 122 mm in November and 152 mm in March), because of a net increase in December $VWC_{0–700}$ of 215 mm from a total precipitation of 232 mm (Table 1). A decrease in ET might be expected in a very wet (and presumably cloudy and relatively cool) month, but 17 mm for ET+*R* in the wet season does not seem reasonable given the apparent availability of soil moisture and the high evaporative demand (72 mm simulated by the model). An examination of the observed VWC of both upper and lower layers and the daily precipitation data (Figure 2) suggests that for much of the November–December period little soil moisture was available in the 0–700-cm layer and that the evaporative demand from 9 November to 5 December may have been partially met by water uptake from the 700–1000-cm soil layer. The largest single-month decrease in observed $VWC_{700–1000}$ of −30 mm (2 times greater than the second largest decrease in May and 15 times greater than the November change) occurs in the 26 days between the November and December measurements (Table 1). Additionally, the rainfall in this period is concentrated in the final 12 days; 200 mm of rainfall (and presumably soil moisture recharge) occurs in the last 12 days before the 5 December $VWC_{0–700}$ measurement, with only 32 mm in the first 14 days (Figure 2). Therefore, it is possible that, because of the very high demand for transpiration and the very low $VWC_{0–700}$ in the early part of the period, root water uptake occurred from below 7 m, which would partially offset the estimated low ET+*R* of the upper layer. In the last 12 days of this period, soil moisture was rapidly recharged and evaporative demand was presumably met from the upper soil layer. The maximum possible ET of 47 mm (17 mm from the upper layer and 30 from the lower layer) is still considerably lower than the simulated evaporative demand of about 72 mm, but it may realistically reflect decreased ET as a result of water stress in the first 14 days, as well as uncertainties in the VWC estimates.

4.4. Spatial variation in volumetric soil water content and its relation with vegetation structure

The large seasonal variation of VWC that was observed during 2005 for transect 2 along depths above 700-cm depth was also observed for the other two measured

locations (sites 1 and 3) during 2003 (Figure 8), indicating that the trend is spatially consistent along the landscape and is a common feature defining the hydrogeology of the area. From 17 February to 15 October 2003, $VWC_{0–700}$ had been considerably reduced in this soil compartment in all transects and the average drop was of 94, 110, and 77 mm for transects at sites 1, 2, and 3, respectively. We observed no further differences for the soil compartment between 700–1000 cm at transect 1 (Figure 8a). We did observe some differences between February and October estimations of $VWC_{700–1000}$ for transects 2 and 3 (Figures 8b,c), with an observed increment in VWC of 14 and 24 mm for transects 2 and 3, respectively, but these differences are relatively small and within the range of those observed during 2005–06 for transect 2.

As was the case for the 2D resistivity profiles (Figure 4), VWC shows a strong spatial pattern of increasing soil water content in the 700–1000-cm depths in transect 2 going from south to north (Figure 8b), which is also present to a lesser extent in transect 1, but absent in transect 3 (Figure 8). These differences show the large heterogeneity of the belowground environment and suggest that geological features determine water distribution in the underground environment. For instance, transect 3 is the wettest site in all soil compartments during both seasons and shows the smallest horizontal variation in VWC along the same profile; and

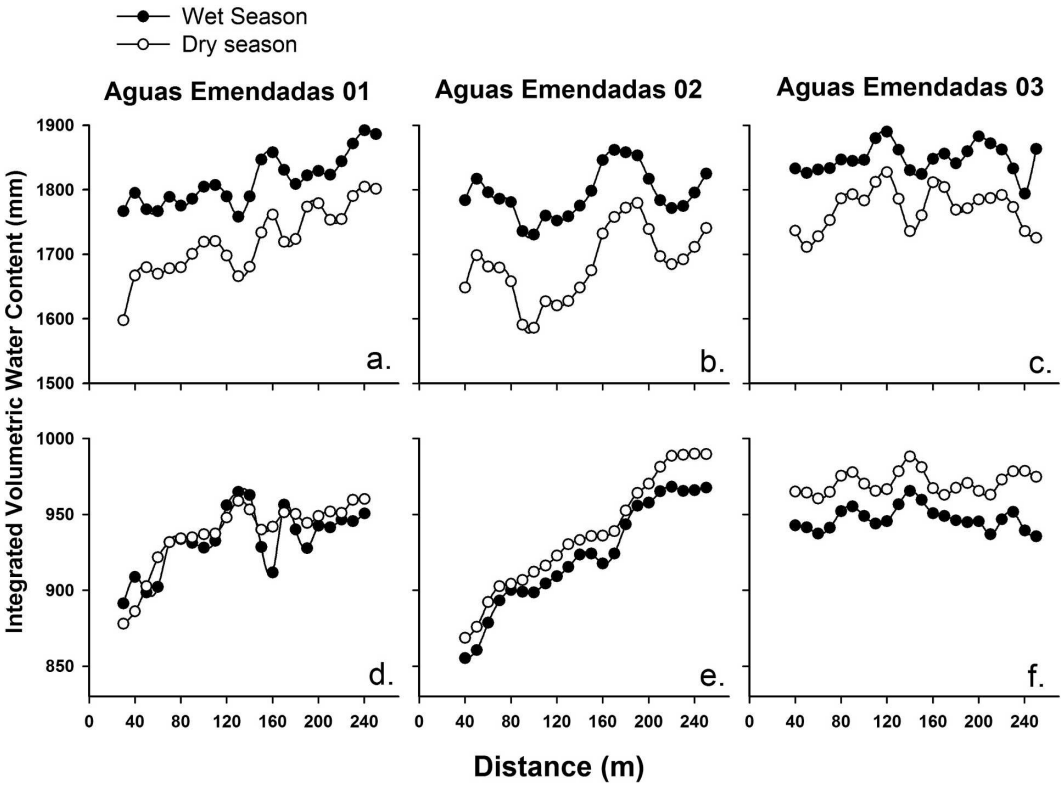

Figure 8. Estimated VWC for the months of February and October of 2003 along three transects located in Águas Emendadas. Values of VWC were summed for intervals of 0–700 and 700–1000 cm.

transect 2 shows the largest horizontal variation of WVC among the three transects, indicating larger spatial heterogeneity in water resources.

The horizontal trends in VWC in 2005–06 along transect 2 were highly correlated with spatial trends observed in vegetation structure, which is consistent with the analysis of the spatial autocorrelation patterns in the 2003 transect data by Ferreira et al. (Ferreira et al. 2007). For example, we found highly significant positive correlations of basal area and plant density with VWC, but the degree of significance varied with soil depth and months of the year. Significant relationships were consistently obtained for basal area with VWC for the 0–300-cm soil layer during May 2005 ($r^2 = 0.638$, $p < 0.001$), December 2005 ($r^2 = 0.569$, $p < 0.05$), and March 2006 ($r^2 = 0.608$, $p < 0.05$)—the wettest months of the year. Tree density was significantly correlated with VWC for the 0–700-cm layer during May 2005 ($r^2 = 0.612$, $p < 0.01$), December 2005 ($r^2 = 0.591$, $p < 0.05$), and March 2006 ($r^2 = 0.582$, $p < 0.05$). Basal area and tree density were greatest where end-of-wet-season VWC was the highest (in May; Figures 9a,b). A positive correlation between basal area and tree density is consistent with the importance of an abundant water resource for the establishment and survival of individuals during the wet season. Neither tree density nor basal area was significantly correlated with VWC in the deepest nonactive soil column.

By contrast, spatial trends in mean crown depth (the distance between the lowest branch and the tree crown top) for each plot was inversely correlated with VWC of all soil depths between 700 and 1000 cm during all the months of the year, except September. Deepest canopies are observed where $VWC_{700–1000}$ was lowest along the transect (Figure 9c). This result is difficult to explain, but we speculate that canopy self-shading in deep canopies of sparsely distributed trees could be an adaptation to areas of low deep soil water resource availability in this ecosystem.

The correlations and observed trends in the structure of the plant community (Figure 9) with VWC suggest that the along-transect differences in soil moisture are quasi-permanent and influence vegetation structure. The spatial–temporal differences in the $VWC_{0–700}$ of transect 2 illustrate this point: the north and south ends of the transect have nearly identical values in May (1936 and 1938 mm, respectively, not shown); by November $VWC_{0–700}$ is reduced by 282 mm in the north end of the transect and only 199 mm in the south end, despite the south end having greater vegetation density, basal area, and presumably evapotranspiration. This much stronger decrease in dry season $VWC_{0–700}$ despite relatively less vegetation suggests greater drainage in the north end of the transect as a result of soil properties.

4.5. Refinement of the 2D resistivity profiling methodology

During this study we used electrode configuration in the Werner array, which has been considered one of the best techniques producing a good signal response and a high resolution of horizontal structures (Ward 1990; Sharma 1997). However, other studies (Seaton and Burbey 2002) have showed that the Werner configuration decreases the resolution of the transition between contact zones of contrasting conductivities and produces more homogeneous low and high resistivity zones of the unconsolidated layers. Future research trying to use this resistivity technology for estimations of soil water content should compare other arrays

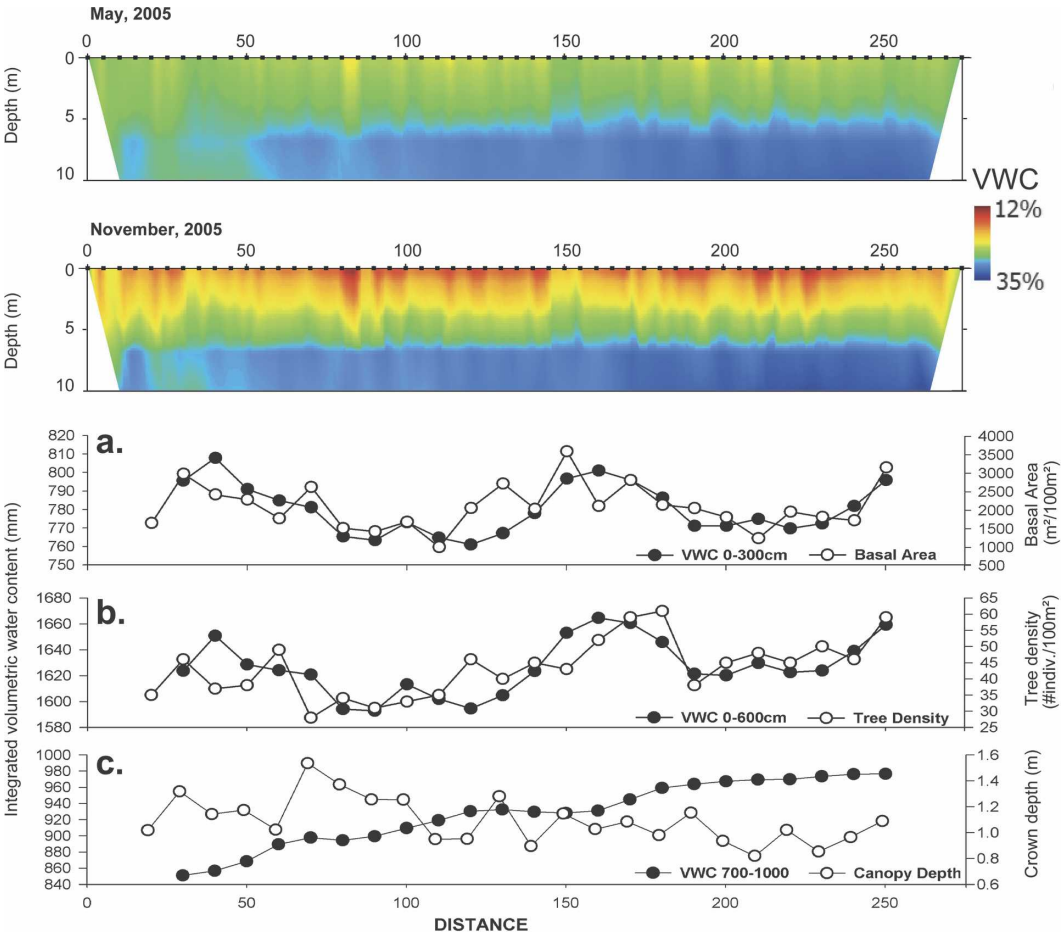

Figure 9. Trends in (a) basal area and $VWC_{0–300}$, (b) tree density and $VWC_{0–700}$, and (c) canopy depth and $VWC_{700–1000}$ in Águas Emendadas. On top the 2D images of the Earth model for *cerrado denso* along transect 2 represent the distribution of VWC after conversion of resistivity values with the equation ln(Resistivity) = 10.882 – 0.004% VWC^2. The resistivity values used to obtain the VWC represented in the 2D images were obtained during measurements conducted at the end of wet season (May 2005). Distance between electrodes was 5 m, and resistivity measurements used a Wenner configuration.

and probably different electrode distances in order to define the minimum resolution needed to obtain the best approximation to the estimates of soil VWC.

Conversion of resistivity values to VWC is dependent on soil type and textural characteristics. Spatial heterogeneity of soil textural characteristics at the scale of tens to hundreds of meters within a single soil type would produce spatial variability in soil water holding properties, thus introducing uncertainties in our calibrations to estimate VWC and plant-available water at the landscape level. More research is needed on how variable these functions may be, not only within an area classified as a single soil type, but among different soil types.

5. Conclusions

The potential role of spatial variation in the belowground water resource on the spatial heterogeneity of aboveground vegetation structure is not obvious from simple aboveground observations of topographic features. At scales of tens to hundreds of meters, such horizontal heterogeneity in the belowground environment is determined by a combination of the distribution of internal structural features, such as thickness of the soil profile, the appearance of abrupt textural changes, the presence of hard pans, the occurrence of impermeable materials, and the fractures in the bedrock, all of which determine niches of soil available water. Such structural features, which help define the geomorphologic characteristics determining soil water availability in this cerrado region, can be visualized, at least in part, through the use of geophysical methods such as the 2D resistivity profiling presented in this study.

This resistivity technology offers the opportunity of quantifying spatial–temporal heterogeneity of water resources, without the need for destructive sampling. Other methods, such as neutron probes and TDR, allow frequent resampling at fixed points, but these measurements are usually more limited in depth and horizontal frequency across the landscape. In contrast to point measurements in individual soil pits, resistivity profiling affords imaging across hundreds of meters horizontally and tens of meters in soil depth, with variation in time, without any difficult soil digging.

Application of resistivity technology to the Águas Emendadas site has given us a much clearer understanding of the spatial–temporal dynamics of plant water uptake and soil characterstics in the cerrado environment. Major findings include 1) the active plant water uptake zone extends to 7-m depth; 2) significant root water uptake occurs before the beginning of the wet season as plants put out new leaves and exhaust the soil moisture stored from the previous wet season; 3) the seasonality of the deep soil compartment (more than 700-cm soil depth) is one order of magnitude less and lags the upper compartment by about 6 months; 4) the deep saturated soil layer may provide modest but important water for evapotranspiration when upper-layer soil water stress reaches a maximum in the late dry/early wet season; and 5) relatively modest differences in soil characteristics play an important role in soil moisture and vegetation structure, where areas of slower soil water drainage are associated with denser vegetation. The knowledge gained in this study will be essential to a better understanding of the response of the hydrology of the cerrado environment to ongoing deforestation and conversion to agriculture.

Acknowledgments. This research was funded by the A. W. Mellon Foundation, the NASA LCLUC program, Grant NNG06GD51G, the NASA LBA project ND-07, and by EPA through the Assistance Agreement 827291-01. The CAPES foreign visiting professor program supported D. Garcia-Montiel during data collection in 2005–06 and a consultancy to the WHRC supported her time during data processing and writing of the manuscript. We thank Mercedes Bustamante for assistance with overall project management and to Carlos Klink and Liliane Bezerra for providing access to TDR data from wells at EEAE. We thank EMBRAPA-Cerrado for laboratory analysis. Peter Schlesinger and Paul Lefebvre provided valuable help with interpolation techniques and comments during data

processing of resistivity. We are grateful to José Eloi Guimarães Campos from the Institute of Geoscience, University of Brasilia, for helping us with the description of the hydrogeology of Águas Emendadas. We would also like to thank Dan Markewitz whose comments helped to improve this paper. Finally, we thank Pedro Simpson, Aylton Lopes Santos, Gilvan Luís de França and Sr. Miguel and the administration of Estação Ecológica de Águas Emendadas for their logistic support.

References

Bucci, S. J., G. Goldstein, F. C. Meinzer, F. G. Scholz, A. C. Franco, and M. Bustamante, 2004: Functional convergence in hydraulic architecture and water relations of tropical savanna trees: From leaf to whole plant. *Tree Physiol.,* **24,** 891–899.

Campos, J. E., 2004: Hidrogeologia do distrito federal: Bases para a gestão dos recursos hídricos subterrâneos. *Rev. Bras. Geocienc.,* **34,** 41–48.

Eastman, J. R., 2003: IDRISI Kilimanjaro. Manual, version 14.002. Clark Labs, Clark University, 244 pp.

EMBRAPA, 1999: Sistema Brasileiro de classificaçao de solos. Centro Nacional de Pesquisa de Solos, Rio de Janeiro, embrapa produção de informação, 412 pp.

Felfili, J. M., and M. C. Silva, 1993: A comparative study of Cerrado (*Sensu stricto*) vegetation in central Brazil. *J. Trop. Ecol.,* **9,** 277–289.

——, ——, A. C. Sevilha, C. W. Fagg, B. M. T. Walter, P. E. Nogueira, and A. V. Rezende, 2004: Diversity, floristic and structural patterns of Cerrado vegetation in Central Brazil. *Plant Ecol.,* **175,** 37–46.

Ferreira, J. N., 2006: Padrões da vegetação lenhosa relacionados à heterogeneidade espacial de água no solo em Cerrado do Brasil Central. Ph.D. dissertation, University of Brasília, 116 pp.

——, M. Bustamante, D. C. Garcia-Montiel, K. Caylor, and E. A. Davidson, 2007: Spatial variation in vegetation structure coupled to plant available water determined by two-dimensional soil resistivity profiling in a Brazilian savanna. *Oecologia,* **153,** 417–430.

Franco, A. C., 2002: Ecophysiology of woody plants. *The Cerrados of Brazil: Ecology and Natural History of a Neotropical Savanna,* P. S. Oliveira and R. J. Marquis, Eds., Columbia University Press, 178–197.

Frost, P., E. Medina, J. C. Menaut, O. Solbrig, M. Swift, and B. Walker, 1986: Responses of savannas to stress and disturbance. *Biol. Int.,* Special Issue 10, 1–78 pp.

Furley, P. A., and J. A. Ratter, 1988: Soil resources and plant communities of the central Brazilian cerrado and their development. *J. Biogeogr.,* **15,** 97–108.

Griffiths, D. H., and R. D. Barker, 1993: Two-dimensional resistivity imaging and modeling in areas of complex geology. *J. Appl. Geophys.,* **29,** 211–226.

Hodnett, M. G., and J. Tomasella, 2002: Marked differences between van Genuchten soil water-retention parameters for temperate and tropical soils: New water-retention pedo-transfer functions developed for tropical soils. *Geoderma,* **108,** 155–180.

——, L. P. Silva, and H. R. Rocha, 1995: Seasonal soil water storage changes beneath central Amazonian rainforest and pasture. *J. Hydrol.,* **170,** 233–254.

Jackson, P. C., and Coauthors, 1999: Partitioning of soil water among tree species in a Brazilian Cerrado ecosystem. *Tree Physiol.,* **19,** 717–724.

Jackson, R. B., and Coauthors, 2005: Trading water for carbon with biological carbon sequestration. *Science,* **310,** 1944–1947.

Jipp, P. H., D. C. Nepstad, and D. K. Cassel, 1998: Deep soil moisture storage and transpiration in forest and pastures of seasonally dry Amazonia. *Climate Change,* **39,** 395–412.

Loke, M. H., and R. D. Barker, 1996: Rapid least-squares inversion of apparent resistivity pseudosections using a quasi-Newton method. *Geophys. Prospect.,* **44,** 131–152.

Lousada, E. O., and J. E. G. Campos, 2006: Proposta de modelos hidrogeológicos conceituais aplicados aos aqüíferos da região do Distrito Federal. *Rev. Bras. Geocienc.,* **35,** 407–414.

Markewitz, D., J. C. F. Resende, L. Parron, M. Bustamante, C. A. Klink, R. O. Figueirdo, and E. A. Davidson, 2006: Dissolved rainfall inputs and streamwater outputs in an undisturbed watershed on highly weathered soils in the Brazilian cerrado. *Hydrol. Processes,* **20,** 2615–2639.

Medina, E., 1993: Mineral nutrition: Tropical savannas. *Prog. Bot.,* **54,** 237–253.

Mente, A., 2000: As condições hidrogeológicas do Brasil. *Hidrogeologia: Conceitos e Aplicações*, Fortaleza: Companhia de Pesquisa e Recursos Minerais (CPRM), Ed., Laboratório de Hidrologia–Universidade Federal de Pernambuco, 323–340.

Moreira, M. Z., F. G. Scholz, S. J. Bucci, L. S. Sternberg, G. Goldstain, F. C. Meinzer, and A. C. Franco, 2003: Hydraulic lift in neotropical savanna. *Funct. Ecol.,* **17,** 573–581.

Motta, P. E. F., N. Curi, and D. P. Franzmeier, 2002: Relations of soils and geomorphic surfaces in the Brazilian Cerrado. *The Cerrados of Brazil: Ecology and Natural History of a Neotropical Savanna,* P. S. Oliveira and R. J. Marquis, Eds., Columbia University Press, 13–32.

Nepstad, D. C., C. R. Carvalho, and E. A. Davidson, 1994: The role of deep roots in the hydrological and carbon cycles of Amazonian forest and pastures. *Nature,* **372,** 666–669.

——, and Coauthors, 2002: The effect of partial throughfall exclusion on canopy processes, aboveground production, and biogeochemistry of an Amazon forest. *J. Geophys. Res.,* **107,** 8085, doi:10.1029/2001JD000360.

Ojelabi, E. A., B. S. Badmus, and A. A. Salau, 2002: Comparative analysis of Wenner and Schlumberger methods of geoelectric sounding in subsurface delineation and ground water exploration—A case study. *J. Geol. Soc. India,* **60,** 623–628.

Oliveira, R. S., L. Bezerra, E. A. Davidson, F. Pinto, C. A. Klink, D. C. Nepstad, and A. Moreira, 2005: Deep root dynamics in Cerrado savannas of central Brazil. *Funct. Ecol.,* **19,** 574–581.

Oliveira-Filho, T. A., G. J. Shepherd, F. R. Martins, and W. H. Stubblebine, 1989: Environmental factors affecting physiognomic and floristic variation in an area of cerrado of central Brazil. *J. Trop. Ecol.,* **5,** 413–431.

Quesada, C. A., A. C. Miranda, M. G. Hodnett, A. J. B. Santos, H. S. Miranda, and L. M. Breyer, 2004: Seasonal and depth variation of soil moisture in a burned open savanna (Campo Sujo) in central Brazil. *Ecol. Appl.,* **14,** S33–S41.

Rawitscher, F., 1948: The water economy of the vegetation of the 'Campos Cerrados' in Southern Brazil. *J. Ecol.,* **36,** 237–268.

Reatto, A., J. R. Correia, and S. T. Spera, 1998: Solos do bioma Cerrado: Aspectos pedológicos. *Cerrado: Ambiente e Flora*, S. M. Sano, and S. P. Almeida, Eds., EMBRAPA-Cerrados, 47–86.

Samouëlian, A., I. Cousin, A. Tabbagh, A. Bruand, and G. Richard, 2005: Electrical resistivity in soil science: A review. *Soil Tillage Res.,* **83,** 173–193.

Seaton, W. J., and T. J. Burbey, 2002: Evaluation of two-dimensional resistivity methods in a fractures crystalline-rock terrace. *J. Appl. Geophys.,* **51,** 21–46.

Shaaban, F. F., and F. A. Shaaban, 2001: Use of two-dimensional electric resistivity and ground penetration radar for archeological prospecting at the ancient capital of Egypt. *J. Afr. Earth Sci.,* **33,** 661–671.

Sharma, P. V., 1997: *Environmental and Engineering Geophysics.* Cambridge University Press, 475 pp.

Sheets, K. R., and J. M. H. Hendrickx, 1995: Noninvasive soil water content using electromagnetic induction. *Water Resour. Res.,* **31,** 2401–2409.

Soil Survey Staff, 1999: *Keys to Soil Taxonomy*. 8th ed. U.S. Department of Agriculture, Soil Conservation Service, 600 pp.

Tabbagh, A., M. Dabas, A. Hesse, and C. Panissod, 2000: Soil resistivity: A non-invasive tool to map soil structure horizonation. *Geoderma,* **97,** 393–404.

Topp, G. C., J. L. Davis, and A. P. Annan, 1980: Electromagnetic determination of soil water content: Measurement in coaxial transmission lines. *Water Resour. Res.,* **16,** 574–582.

Van Genuchten, M. T., 1980: A closed-form equation for predicting the hydraulic conductivity of unsaturated soils. *Soil Sci. Soc. Amer. J.,* **44,** 892–898.

Ward, S. H., 1990: Resistivity and induced polarization methods. *Geotechnical and Environmental Geophysics,* S. H. Ward, Ed., Vol. 1, Society of Exploration Geophysicists, 147–189.